Heterogeneous OH Initiated Oxidation: A Possible Explanation for the Persistence of Organophosphate Flame Retardants in Air

ARTICLE *in* ENVIRONMENTAL SCIENCE & TECHNOLOGY · JANUARY 2014

Impact Factor: 5.33 · DOI: 10.1021/es404515k · Source: PubMed

6 AUTHORS, INCLUDING:

Yongchun Liu
Chinese Academy of Sciences
53 PUBLICATIONS **529** CITATIONS
SEE PROFILE

Tom Harner
Environment Canada
203 PUBLICATIONS **11,372** CITATIONS
SEE PROFILE

Mahiba Shoeib
Environment Canada
59 PUBLICATIONS **3,716** CITATIONS
SEE PROFILE

Environmental Science & Technology

Article

pubs.acs.org/est

Heterogeneous OH Initiated Oxidation: A Possible Explanation for the Persistence of Organophosphate Flame Retardants in Air

Yongchun Liu, John Liggio,* Tom Harner, Liisa Jantunen, Mahiba Shoeib, and Shao-Meng Li

Atmospheric Science and Technology Directorate, Science and Technology Branch, Environment Canada, Toronto, M3H 5T4, Canada

Supporting Information

ABSTRACT: Heterogeneous reactions between OH radicals and emerging flame retardant compounds coated on inert particles have been investigated. Organophosphate esters (OPEs) including triphenyl phosphate (TPhP), tris-2-ethylhexyl phosphate (TEHP), and tris-1,3-dichloro-2-propyl phosphate (TDCPP) were coated on $(NH_4)_2SO_4$ particles and exposed to OH radicals in a photochemical flow tube at 298 K and (38.0 ± 2.0) % RH. The degradation of these particle-bound OPEs was observed as a result of OH exposure, as measured using a Time-of-Flight Aerosol Mass Spectrometer. The derived second-order rate constants for the heterogeneous loss of TPhP, TEHP, and TDCPP were $(2.1 \pm 0.19) \times 10^{-12}$, $(2.7 \pm 0.63) \times 10^{-12}$, and $(9.2 \pm 0.92) \times 10^{-13}$ cm^3 molecule^{-1} s^{-1}, respectively, from which approximate atmospheric lifetimes are estimated to be 5.6 (5.2−6.0), 4.3 (3.5−5.6), and 13 (11−14) days. Additional coating of the OPE coated particles with an OH radical active species further increased the lifetimes of these OPEs. These results represent the first reported estimates of heterogeneous reaction rate constants for these species. The results demonstrate that particle bound OPEs are highly persistent in the atmosphere with regard to OH radical oxidation, consistent with the assumption that OPEs can undergo medium or long-range transport, as previously proposed on the basis of field measurements. Finally, these results indicate that future risk assessment and transport modeling of emerging priority chemicals with semi- to low-volatility must consider particle phase heterogeneous loss processes when evaluating environmental persistence.

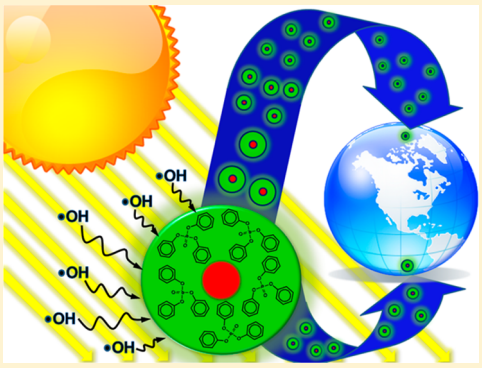

1. INTRODUCTION

Organophosphate esters (OPEs) have been used extensively worldwide as flame retardants, plasticizers, antifoaming agents, and additives.[1] In 2005, the global amount of OPEs used as flame retardants was 270 000 tons.[2] Although tris-2-chloroethyl phosphate (TCEP) has been phased out in Europe and is being phased out in Canada, the global consumption of OPEs is expected to increase since they have been identified as possible substitutes for some bromine-containing flame retardants (BFRs).[3,4]

In most applications, OPEs are additives and not chemically bonded to a given material, and hence are easily emitted into the environment via volatilization, abrasion, and dissolution.[5] Consequently, OPEs have frequently been detected in surface waters,[6,7] sediments,[7] soil,[8] snow,[1] and airborne particles.[9] For example, the concentrations of various OPEs, including tris-ethyl phosphate (TEP), TCEP, tris-2-chloro-1-propyl phosphate (TCPP), triphenyl phosphate (TPhP), tris-1,3-dichloro-2-propyl phosphate (TDCPP), tributyl phosphate (TBP), and tris-2-butoxyethyl-phosphate (TBEP) ranged from tens to several thousand ng L^{-1} in lakes and rivers across Europe.[6,7,10−12] In the atmosphere, TCEP, TCPP, TDCPP, TBP, TBEP, TPhP, and tris-2-ethylhexyl phosphate (TEHP) have frequently been detected in indoor suspended dust and ambient airborne particles.[4,9,13,14] Möller et al. found in ambient air that the sum of the measured OPEs ranged from 230 to 2900 pg m^{-3} in samples varying latitudinally from East Asia to the high Arctic, and from 120 to 1700 pg m^{-3} from East Asia to the Antarctic.[9] These are higher than the levels of BFRs in indoor air, dust, and ambient air.[15]

In the atmosphere, reaction with the OH radicals is expected to be the dominant atmospheric loss process for the OPEs.[16,17] Their second-order gas-phase reaction rate constants (k_2) with respect to OH vary from 10^{-12} to 10^{-10} cm^3 molecule^{-1} s^{-1} calculated using the Atmospheric Oxidation Program (AOP) model.[18] Currently, the risk to humans and ecosystems associated with the widespread production and use of OPEs is assessed through modeling of the fate of these species in various environmental media.[16,19] In estimating the atmospheric fate of OPEs, gaseous OH radical rate constants are widely accepted as inputs in risk assessment modeling of OPEs.[16] Using such kinetic data, the atmospheric lifetimes for OPEs are estimated to be less than 1.3 days. For example, the estimated lifetime for TEHP via the reaction with OH radicals is 3 h.[19] However, many OPEs, such as TCEP, TCPP, TDCPP,

Received: October 9, 2013
Revised: December 18, 2013
Accepted: December 23, 2013

TBP, TBEP, TEHP, and TPhP, are predominantly associated with airborne particles[14,15] and have been measured in polar regions. This implies that OPEs are persistent in air and can undergo medium to long-range transport [9] over days to weeks. Consequently, the rate constants for the degradation of these compounds in the particle phase must be smaller than for the gas phase, which have been used in assessing the atmospheric persistence of these species. What is needed for a more accurate assessment of the atmospheric lifetimes of these OPEs is the kinetic data for the degradation of OPEs in the particle phase, which is currently unavailable.

In this work, the OH radical initiated heterogeneous reaction kinetics of TPhP, TEHP, and TDCPP coated on $(NH_4)_2SO_4$ were investigated using a photochemical flow tube coupled to an Aerodyne Research Incorporated compact time-of-flight aerosol mass spectrometer (C-ToF-AMS) and an Ionicon Analytik proton transfer reaction mass spectrometer (PTR-MS). The heterogeneous rate constants (k_2) for these compounds with respect to OH were measured at 298 K, from which the atmospheric lifetimes were calculated.

2. EXPERIMENTAL SECTION

A detailed schematic representation of the experimental system utilized in this study is shown in the Supporting Information, SI, Figure S1. Ammonium sulfate ($(NH_4)_2SO_4$) particles were generated via atomization (model 3706, TSI), dried through a diffusion drier, and size-selected with a differential mobility analyzer (DMA) (model 3081, TSI) to have a mode mobility diameter (D_m) of approximately 100 nm. The monodispersed particles then passed through a Pyrex tube containing the liquid OPE of interest, which was heated to between 343 and 358 K depending upon the vapor pressure of OPE. The temperature was chosen to ensure a coated particle D_m of ∼180 nm. The coated particles (denoted OPE−AS) were introduced into a mixing vessel after having passed through an activated carbon denuder to remove volatile organics vapors from the flow. In order to investigate the influence of mixing state on the reaction kinetics, the OPE−AS particles were further coated with oxalic acid (denoted as Oxa−OPE−AS) prior to entering a photochemical reactor (see SI Figure S1).

OH radicals were produced by the photolysis of O_3 at 254 nm in the presence of water vapor. O_3 was generated by passing zero air through an O_3 generator (OG-1, PCI Ozone Corp.). O_3 concentration in the reactor was measured using an O_3 monitor (model 205, 2B Technologies) and ranged from 0 to 1000 ppbv. Relative humidity (RH) in the reactor was kept constant (38.0 ± 2.0) % by adjusting the ratio of wet to dry air used as an air source, and was measured at the exit of the reactor.

OH radical reactions were performed in a custom-made reactor (7.3 cm I.D. × 25 cm L.) (SI Figure S2) consisting of two electro-polished stainless steel cylinders. The first stage contained static mixing elements (StaMixCo Inc.) to ensure that particles and gas phase species were well mixed prior to entering the reaction region (second stage). Fluid dynamics simulations of the flow tube setup confirmed that particles and gas phase species were well mixed in the reactor, with a uniform initial velocity profile. The flow rate was 1.1 L min^{-1} with a residence time of ∼52 s. Further details regarding the photochemical reactor design and operation is given in the SI (Figure S2).

The steady-state OH radical concentrations were measured during each experiment using methanol as a reference compound. The decay of methanol from its reaction with OH (9.4×10^{-13} cm^3 $molecule^{-1}$ s^{-1} at 298 K [20]) was measured using the PTR-MS, and corresponded to an OH radical concentration in the reactor spanning the range of 0 to ∼1.5×10^{10} molecules cm^{-3}.

The concentration, size, and composition of the particles exiting the reactor were measured by a scanning mobility particle sizer (SMPS, TSI) and the C-ToF-AMS.[21] The kinetics of the heterogeneous oxidation of OPEs by OH was investigated by measuring the loss of particle phase OPEs as a function of the OH exposure. Control experiments demonstrated that O_3 exposure did not lead to the decomposition of OPEs. To exclude the possible influence of OPE photolysis by the 254 nm light on these kinetic studies, the particles were illuminated to measure the initial concentration prior to O_3 introduction. TPhP, TDCPP, and TEHP (TCI America Inc.) were used in these experiments and their chemical structures are shown in Figure 1.

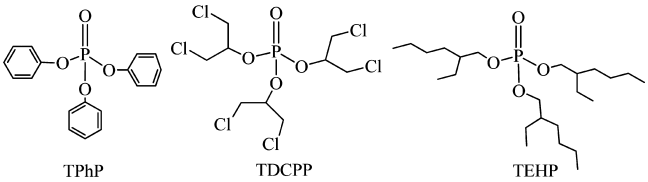

Figure 1. Structures of OPEs investigated in this study.

3. RESULTS AND DISCUSSION

3.1. Degradation of OPE−AS. The degradation of particle bound OPEs are observable via the C-ToF-AMS measurements during a given experiment. The typical mass spectra of unreacted and reacted TPhP, TEHP, and TDCPP coated on $(NH_4)_2SO_4$ particles are shown in Figure 2. The left column (green color) and the middle column (red color) represent unreacted OPEs and oxidized OPEs, respectively. The right column is the corresponding difference mass spectrum (reacted−unreacted). For these three OPEs, their fragmentation patterns measured with the C-ToF-AMS are comparable with those in the NIST database (SI Figure S3) and since the three OPEs utilized contain distinctly different functional groups (Cl, phenyl, hydrocarbon) their respective unreacted and degradation C-ToF-AMS fragments are distinctly different.

As shown in Figure 2, fragments at m/z of 326, 233, 140, and 77 for TPhP are observable, which correspond to $(C_6H_5O)_3PO^+$, $(C_6H_5O)_2PO^+$, $C_6H_5OPO^+$, and $C_6H_5^+$, respectively, while the ion at m/z 326 is the molecular ion of TPhP. When TPhP−AS particles were exposed to OH radicals, the normalized intensities of the above fragments decreased substantially (Figure 2). Concurrently, the fragments at m/z 342 and 249 increased as shown in the inset graph of Figure 2 and were ascribed to the oxidation product ($(C_6H_5O)_2PO(OC_6H_5O)^+$; m/z 342) and its associated fragmentation ($(C_6H_5O)PO(OC_6H_5O)^+$; m/z 249). This is indicative that a radical addition reaction occurred for the TPhP oxidation, consistent with the well-known mechanism of OH radical addition to aromatic hydrocarbons [20] which is dominant over hydrogen abstraction for such compounds.

Conversely, the C-ToF-AMS spectrum for oxidized TEHP and TDCPP do not contain fragments greater than their respective molecular ions (m/z 435 and 431). Oxidation of TEHP result in spectra that are consistent with the oxidation of

dx.doi.org/10.1021/es404515k | Environ. Sci. Technol. XXXX, XXX, XXX−XXX

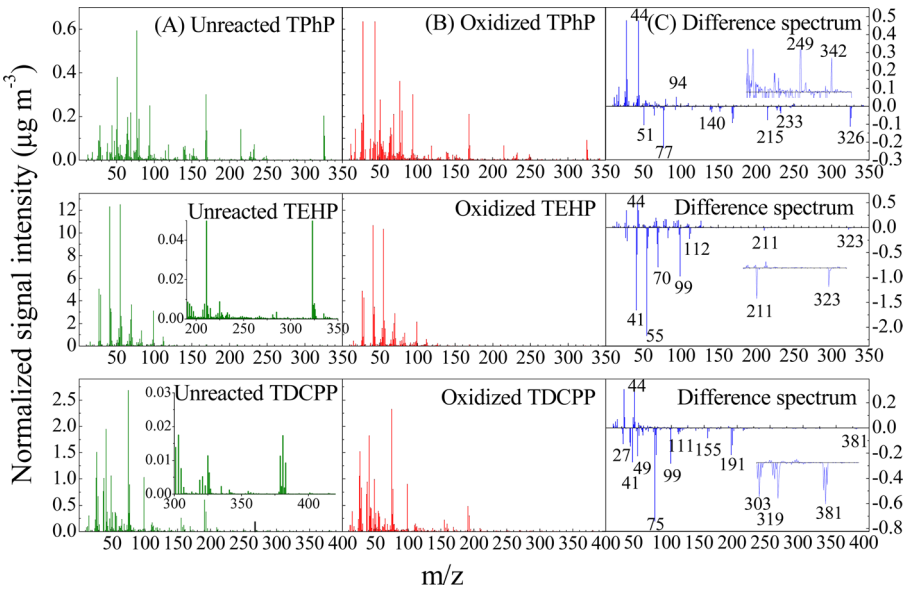

Figure 2. Mass spectra of (A) unreacted OPE, (B) oxidized OPE at OH exposure of 4.5, 3.3, and 4.9 × 10^{11} molecules cm^{-3} s, respectively, and (C) difference mass spectra between the oxidized and unreacted OPE; the inset graphs show the corresponding magnified area.

saturated hydrocarbon compounds, leading to a series of hydrocarbon fragments that decrease with OH exposure.[20] These include, *m/z* 27, 29, 41, 43, 55, 57, 69, 83, and 99 (Figure 2D), which correspond to $C_2H_3^+$, $C_2H_5^+$, $C_3H_5^+$, $C_3H_7^+$, $C_4H_7^+$, $C_4H_9^+$, $C_5H_9^+$, $C_6H_{11}^+$, and $C_7H_{15}^+$. The presence of chlorinated ester functional groups in TDCPP result in distinctive fragments at *m/z* 49, 75, 111, 155, 191, 303, 319, and 381 corresponding to CH_2Cl^+, $CH_2ClCCH_2^+$, $CH_2ClCCH_2Cl^+$, $(CH_2CHCH_2ClO)PO_2^+$, $(CH_2ClCHCH_2ClO)PO_2^+$, $(CH_2ClCHCH_2ClO)_2PO^+$, $(CH_2ClCHCH_2ClO)_2PO_2^+$, and $(CH_2ClCHCH_2ClO)_2PO(OCHCH_2Cl)^+$. For both TEHP and TDCPP, their molecular ion peak at *m/z* of 435 and 431 cannot be detected with electron impact ionization at 70 eV. However, the decrease in the signals of other fragments as noted above with OH exposure is representative of a heterogeneous loss process for all three species. The implications of these fragments on the derived heterogeneous kinetics are discussed further below.

3.2. Kinetics of OPEs Degradation. The ability to derive kinetic information for the heterogeneous degradation of various OPEs is dependent upon the ability to (1) quantify the OH radical concentration in the reactor using methanol as a tracer, (2) observe relative changes in OPE signal with OH exposure, and (3) reproducibly generate a constant stream of particles. Some of these requirements are demonstrated in Figure 3, which depicts the response of TPhP and methanol concentration to OH exposure. In the presence of OH radicals, TPhP in the particle phase and the gaseous methanol tracer were clearly oxidized. In varying OH exposure from 8.1 × 10^{11} to 1.9 × 10^{11} molecules cm^{-3} s in Figure 3, the concentrations of TPhP and methanol changed synchronously within experimental uncertainties. Most notably, at the end of a given exposure cycle and with no OH radical present (160−180 min, Figure 3), both the molecular ion signals for TPhP and the methanol concentration recover to their initial values. This indicates that memory effects are negligible and that kinetic parameters can be reliably derived.

In typical flow tube experiments, the signals for particle phase species (as measured by AMS in this study) are often

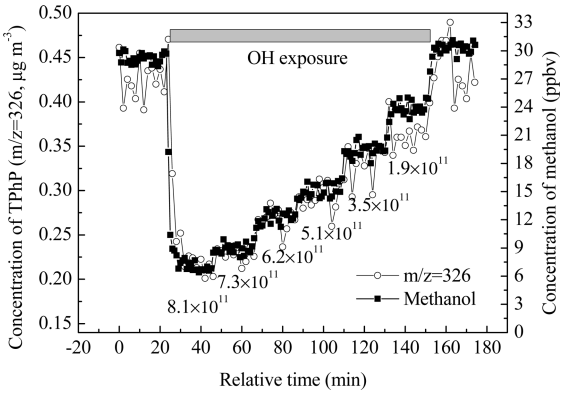

Figure 3. Response of TPhP and methanol concentration to OH exposure. Values in plot are derived average OH radical concentration in molecules cm^{-3} s.

normalized by particle number concentration in order to compensate for variations in the stability of particle generation.[21] However, the OPEs investigated in this study are semivolatile organic compounds (SVOCs). The vapor pressures of TPhP, TEHP, and TDCPP at 298 K are 1.6 × 10^{-4}, 2.7 × 10^{-4}, and 9.8 × 10^{-6} Pa (SI Table S1),[22] respectively, which corresponds to a *C** (*C**= *P/RT*) of 21, 47, and 1.7 $\mu g\ m^{-3}$. Consequently, despite the use of an activated carbon denuder prior to the particles entering into the reactor, a small amount of gas phase OPEs cannot be avoided in the reactor, which may oxidize and lead to new particle formation. Although not sampled into the AMS due to their sub-10 nm size and their negligible mass, their presence precludes the normalization of the OPE signal by the particle number concentration. Alternatively, the OPE signal can be normalized to the SO_4 signal. However, under these conditions, the SO_4 signal included a significant OPE interference. Therefore, a stable source of OPE mass (coated on inorganic seed particles) is required for the entire experiment. SI Figure S4 shows the molecular ion signal of TPhP−AS measured with the C-ToF-AMS under experimental conditions. From SI Figure S4, it is evident that the particle source is stable within experiment

dx.doi.org/10.1021/es404515k | Environ. Sci. Technol. XXXX, XXX, XXX−XXX

uncertainties and for the time required to complete a given experiment. A stable particle source is also demonstrated by the recovery of the TPhP signal in the absence of OH radical as shown in Figure 3. In addition, oxidation experiments were performed at a constant flow, with constant particle wall losses. Consequently, the non-normalized C-ToF-AMS signals were used for deriving kinetic parameters since wall losses should have no influence on the kinetic calculation.

It should be noted that if the gas phase OH reaction of OPE is faster than that in the particle phase, evaporation of OPE from particles could potentially contribute to the decreases in particle phase OPE concentration observed as a function of OH exposure (i.e., Figure 3) via the establishment of a new gas-particle equilibrium. The extent to which this process interferes with the derived kinetics will depend upon the amount in the gas phase relative to particle phase, and the ability of the OPE to evaporate from the particles on the time scales of the experiment. In order to ensure that changes in gas-particle equilibrium are not substantially affecting the perceived heterogeneous oxidation, experiments were performed whereby the activated carbon denuder was bypassed (under dark conditions). As demonstrated in SI Figure S5, there is no difference in OPEs C-ToF-AMS signal in the presence or absence of the carbon denuder. This is consistent with other studies which show that equilibrium time scales for gas-particle partitioning are rather large.[23,24] These results indicate that evaporation of the OPEs from particles has a negligible influence on the OPEs concentration in particle phase, and likely even less so for TDCPP given its lower vapor pressure.

Assuming a second order reaction between OH and OPEs, the loss rate of OPEs can be expressed as follows:

$$-\frac{d[\mathrm{OPEs}]}{dt} = k_2[\mathrm{OH}][\mathrm{OPEs}] \quad (1)$$

where k_2 is the second-order rate constant of OPEs (cm^3 $molecule^{-1}$ s^{-1}), [OH] is the gas phase concentration of OH radicals (molecules cm^{-3}), and [OPEs] is the concentration of OPEs (molecules cm^{-2}). Since the experiments were performed under steady state conditions with constant OH concentrations, eq 1 can be integrated from zero to the residence time (t) of reactants.

$$\ln\frac{[\mathrm{OPEs}]}{[\mathrm{OPEs}]_0} = \ln\frac{I}{I_0} = -k_2[\mathrm{OH}]t \quad (2)$$

where $[\mathrm{OPEs}]_0$ represents the initial concentration of OPEs, I and I_0 are signal intensities for the mass spectral tracers (proportional to the OPE concentration) in the presence and absence of OH radical.

The changes in I/I_0 for TPhP−AS, TEHP−AS, and TDCPP−AS as a function of OH exposure at 298 K are shown in Figure 4. Colored data points represent independent experiments, and the lines are exponential curve fitting results from which second order rate constants (k_2) are derived via eq 2. The second-order rate constants are shown in Table 1 with the uncertainties represented as the standard derivations (σ) for five sets of experiments. The measured k_2 were corrected for gas phase diffusion by applying a previously utilized empirical formula.[25,26] The measured k_2 for TPhP−AS was $(1.6 \pm 0.17) \times 10^{-12}$ cm^3 $molecule^{-1}$ s^{-1}, which was calculated from the decay of the molecular ion at m/z 326. The measured k_2 for TEHP−AS and TDCPP−AS were $(2.1 \pm 0.55) \times 10^{-12}$ and

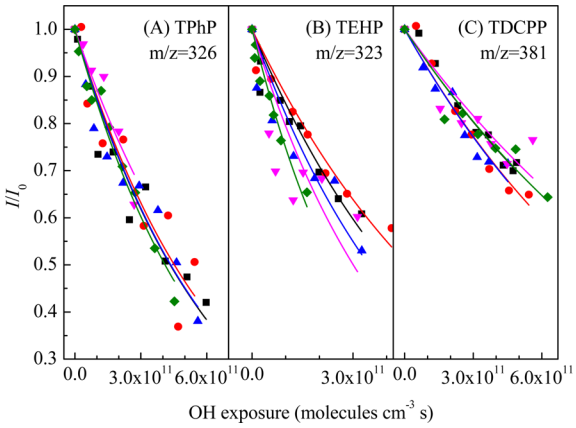

Figure 4. Signal intensity fractions for fragments representative of (A) TPhP, (B) TEHP, and (C) TDCPP coated on $(NH_4)_2SO_4$ as a function of OH exposure at 298 K. The color series indicate independent experiments.

$(7.7 \pm 0.86) \times 10^{-13}$ cm^3 $molecule^{-1}$ s^{-1} based upon the decays of m/z of 323 and m/z 381, respectively.

It should be pointed out that there were many fragments for each OPE which decreased with OH exposure, as shown in Figure 2. Although a decrease with OH exposure does indicate a degree of heterogeneous processing, it is possible that oxidation products (and subsequent smaller m/z fragments) may contain the same MS fragments which depress the observed decay rates in Figure 4. Under such a scenario, the result would be a possible underestimation of k_2. For example, as shown in Table 1, k_2 values based upon the fragments at m/z of 233, 140, and 77 for TPhP are $(1.3 \pm 0.13) \times 10^{-12}$, $(6.2 \pm 0.11) \times 10^{-13}$, and $(8.1 \pm 0.45) \times 10^{-13}$ cm^3 $molecule^{-1}$ s^{-1}, respectively. The k_2 values calculated on the basis of m/z = 140 and 77 are smaller than the k_2 calculated from the decay of the molecular ion peak of TPhP (m/z = 326). Since the molecular ions for TEHP and TDCPP are undetectable with the ToF-AMS, we calculated k_2 using their largest mass fragment observable, namely, m/z of 323 for TEHP and m/z 381 for TDCPP. Consequently, k_2 for these two species may be slightly underestimated.

At the present time, experimental or theoretical kinetic data for OPE reactivity with OH radicals are very limited. To the best of our knowledge, no previous studies have investigated the kinetics of OPE degradation on particle surfaces, with only a few reports of OH reaction kinetics available for other media such as water or gas phase,[17,27−32] as summarized in Table 2. Generally, the k_2 of TPhP and TEHP in particle phase here is lower than other aryl-phosphates in the gas and water phase, while the k_2 of TDCPP in the particle phase is comparable to that of other chloro alkyl phosphates in water. The lower reactivity of TDCPP relative to TPhP and TEHP is consistent with the lower reactivity of other chloro alkyl phosphates in water.[30−32]

The k_2 for OPEs have also been estimated using the AOPWIN model and are summarized in Table 2. The AOPWIN model,[18] which is based upon structure−activity relationship (SAR) methods developed by Atkinson and co-workers,[20,33] has been widely used to predict the rate constants for atmospheric gas-phase reactions between organic molecules and OH radicals. The predicted k_2 values agree very well with the experimental data for gas-phase reactions, with uncertainties of 15% as shown in Table 2. However, the model overestimates

dx.doi.org/10.1021/es404515k | Environ. Sci. Technol. XXXX, XXX, XXX−XXX

Table 1. Reaction Kinetics of TPhP, TEHP, and TDCPP Coated on $(NH_4)_2SO_4$ at 298 K

OPE	m/z	k_2 (10^{13} cm^3 molecule^{-1} s^{-1}) exp 1	exp 2	exp 3	exp 4	exp 5	average $k_{2,obs}$	diffusion corrected k_2	γ_{OH}
TPhP	77	8.4	8.3	7.6	7.4	9.9	8.1 ± 0.45		
	140	6.1	6.2	6.3	4.5	8.3	6.2 ± 0.11		
	233	13	15	12	12	13	13 ± 1.3		
	326	16	17	14	16	16	16 ± 1.7	21 ± 1.9	0.70 ± 0.07
TEHP	323	17	15	20	29	23	21 ± 5.5	27 ± 6.3	0.65 ± 0.27
TDCPP	381	7.3	6.8	8.7	8.6	7.3	7.7 ± 0.86	9.2 ± 0.92	0.39 ± 0.03

Table 2. Comparisons between measured and estimated k_2 and lifetimes for OPEs

OPs	k_2 (cm^3 molecule^{-1} s^{-1}) laboratory	AOPWIN	atmospheric lifetime (days) laboratory	AOPWIN
TMP	$7.4 \times 10^{-12,a}$	8.4×10^{-12}	1.6	1.3
TEP	$(5.1 \pm 0.3) \times 10^{-11,b}$	5.8×10^{-11}	0.2	0.2
TCEP	$9.3 \times 10^{-13,c}$	2.2×10^{-11}		0.5
TCPP	$3.3 \times 10^{-13,c}$	4.5×10^{-11}		0.3
TBEP	$1.7 \times 10^{-11,c}$	1.3×10^{-10}		0.1
TnBP	$1.1 \times 10^{-11,c}$	7.9×10^{-11}		0.1
TPhP	$(2.1 \pm 0.19) \times 10^{-12,d}$	1.1×10^{-11}	5.6(5.2−6.0)	1.1
TEHP	$(2.7 \pm 0.63) \times 10^{-12,d}$	9.8×10^{-11}	4.3(3.5−5.6)	0.1
TDCPP	$(9.2 \pm 0.92) \times 10^{-13,d}$	1.8×10^{-11}	13(11−14)	0.6

[a]In gas phase, Tuazon et al.[27] [b]In gas phase, Aschmann et al.[17,28] [c]In aqueous phase, calculated based on Watts and Linden's results.[32] [d]In particle phase, this study. TMP: tris-methyl phosphate; TEP: tris-ethyl phosphate; TCEP: tris-2-chloroethyl phosphate; TCPP: tris-chloroisopropyl phosphate; TBEP: tris-2-butoxyethyl phosphate; TnBP: tris-*n*-butyl phosphate; TPhP: tris-phenyl phosphate; TEHP: tris-2-ethylhexyl phosphate; TDCPP: tris-1,3-dichloro-2-propyl phosphate.

the k_2 for these OPEs in the condensed phase by approximately an order of magnitude, suggesting that SAR methods might not be suitable for predicting the rate constants of OPEs in the particle phase, which are often used to assess the atmospheric fate of these species.

The reactive uptake coefficient of OH (γ_{OH}) with OPs-AS was calculated using the following formulation:[26,34−36]

$$\gamma_0 = \frac{2D_p\rho_{OPEs}N_A}{3v_{OH}M_{OPEs}}k_2 \quad (3)$$

where D_p is the surface-weight average particle diameter of unreacted particles (cm), ρ_{OPEs} is the density of OPEs (g cm^{-3}), N_A is Avogadro's number, v_{OH} is the average speed of OH radicals in the gas phase (cm s^{-1}), M_{OPEs} is the molecular weight of OPEs (g mol^{-1}). The diffusion-corrected γ_{OH} on OPEs − AS particles is shown in Table 1. Values of γ_{OH} on a number of different organic particles have previously been measured, and are in the range of 0.3 − 2.0.[21,34,35,37−39] Our results are of the same order of magnitude as these previous measurements of OH uptake coefficients.

3.3. Kinetics of Oxa−OPEs−AS. In the ambient atmosphere, particles are often internally or externally mixed with many other components, and it is well recognized that the mixing state or morphology of particles plays an important role in heterogeneous reaction kinetics.[40−43] In order to understand the possible influence of other components on the OH reactivity of OPEs, TPhP−AS was further coated with oxalic acid prior to OH exposure. Oxalic acid was chosen as a third aerosol component since (1) oxalic acid is the most abundant organic acid present in atmospheric particles,[44−46] and (2) the vapor pressure of oxalic acid is ideal for further condensation on TPhP−AS particles without significant evaporation of TPhP.

The change in the diffusion-corrected k_2 of TPhP as a function of the estimated thickness of oxalic acid coated on TPhP−AS particles is shown in Figure 5. The diffusion-corrected k_2 nonlinearly decreased with increasing thickness of oxalic acid coating, and was approximately constant when coated with greater than 10 nm of oxalic acid. $(NH_4)_2SO_4$, TPhP, and oxalic acid contribute ∼15%, 50%, and 35%, respectively, to the total mass for 10 nm of oxalic acid coated Oxa−TPhP−AS particles. An example of the surface-weighted size distribution for TPhP−AS and Oxa−TPhP−AS particles as well as the corresponding change of TPhP fractions as a function of OH exposure is given in SI Figure S6. Compared with the uncoated reference (Table 1), the k_2 of TPhP decreased by a factor of 2.6 for Oxa−TPhP−AS particles with a thickness of oxalic acid greater than 10 nm.

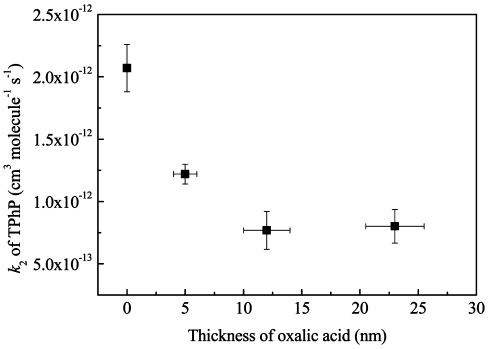

Figure 5. Diffusion-corrected k_2 for TPhP as a function of the thickness of oxalic acid coated on TPhP−AS particles.

Such results are similar to those observed for ozonolysis of organic aerosols. For example, Zhou et al. [47] found that the

dx.doi.org/10.1021/es404515k | Environ. Sci. Technol. XXXX, XXX, XXX−XXX

heterogeneous reactivity of benzo[α]pyrene toward O_3 was reduced substantially by an eicosane coating. In particular, it decreased to zero with a thick coating of eicosane (15−20 nm). However, unlike the results of Zhou et al, consumption of TPhP was still observed with a thick coating of oxalic acid. This difference can be explained by differences in reactivity between the oxidants and the coated compounds. In their work, eicosane is chemically inert to ozone, whereas OH is active to virtually all organic compounds including TPhP and oxalic acid. This suggests that TPhP will ultimately be exposed to OH after oxalic acid has been partially or fully consumed. On the other hand, we assume oxalic acid was evenly coated on the TPhP−AS particles to form an ideal core−shell structure. However, we have no evidence that this was indeed the case, and it is possible that oxalic acid was not evenly distributed on the surface or internally mixed. In this case, the reaction between TPhP and OH radicals may not have been completely inhibited. Therefore, it is likely that both diffusion of OH through an organic film as well as the competitive reaction between OH and oxalic acid reduce the reactivity of TPhP toward OH.

4. IMPLICATIONS

The current results have important implications for the fate of OPEs in the atmosphere and for the methods by which new and emerging compounds are risk-assessed. The atmospheric persistence of OPEs can be expressed as a lifetime (τ), which are calculated using the diffusion-corrected rate constants via eq 4.

$$\tau = \frac{1}{k_2[\mathrm{OH}]} \quad (4)$$

Assuming a 24 h average OH concentration of 1.0×10^6 molecules cm^{-3},[48] the lifetimes of TPhP, TEHP, and TDCPP were estimated to be 5.6 (5.2−6.0), 4.3 (3.5−5.6), and 13 (11−14) days (Table 2), respectively. The lifetimes of TMP and TEP with respect to OH oxidation in the gas-phase were also calculated based upon their measured[17,28] and AOPWIN modeled rate constants (Table 2). While the measured and modeled gas phase lifetimes for TMP and TEP are comparable, they are substantially shorter than the particle phase lifetimes derived for similar compounds in this study. This suggests that those OPEs which are predominantly in the condensed phase will be much more persistent than those in the gas phase. A calculated particle phase lifetime on the order of days to weeks is consistent with the presence of particle bound OPEs in polar regions.[9,14] If the reaction with OH is the primary route for particulate OPE degradation in the atmosphere, then our results might well explain the medium-range [9] or long-range transport [14] observed for this class of compounds. It should be pointed out that OPEs are semivolatile compounds (SVOC). Evaporation from particles will affect the overall atmospheric lifetime for these compounds. To fully understand their atmospheric behavior, a model incorporating evaporation, gas phase, and heterogeneous degradation is required. Recent studies[49] also suggest that mass transfer limitations due to the phase of atmospheric particles (i.e., semi-solid) will significantly increase the time required for the establishment of gas-particle equilibrium. This would imply that the overall atmospheric lifetime for OPEs may be governed by heterogeneous oxidation.

In addition, the particle lifetimes derived here will likely be a lower limit given the complex mixing state of ambient particles, and the observed decrease in the second order rate constant as a result of oxalic acid coating here. For example, when TPhP−$(NH_4)_2SO_4$ particles were further coated with ∼20 nm of oxalic acid, the lifetime of TPhP increased from 5.6 to 14 (12−17) days. A complex ambient mixture will likely have a similar effect and further increase the persistence of these species. In particular, Hennigan et al. [50] have observed a decrease in reactivity of levoglucosan toward OH in wood smoke compared to pure levoglucosan. Such a substrate effect of black carbon on OPEs might also have a negative influence on the OPEs degradation rate. The experiments were only performed at one temperature and RH. All of these factors will likely affect the reactivity of OPEs and requires further investigation.

Finally, risk assessments for new and emerging priority compounds are often performed using modeled rate constants.[16] The modeled lifetimes of TPhP, TEHP, and TDCPP based upon SAR kinetic data range from 0.1 to 1.1 days (Table 2). However, the measured particle phase lifetimes in the current study are substantially longer, suggesting that a proper assessment of the atmospheric persistence of these species requires a more complete understanding of heterogeneous oxidation processes, and the use of experimentally derived rate constants rather than modeled parameters. This new information will also greatly improve our ability to model the fate and transport of particle-bound priority chemicals so that predictions can be reconciled with monitoring data. The results demonstrate an enhanced atmospheric persistence for OPEs that are associated with particles that can provide a realistic mechanism to account for their abundance in remote atmospheres such as over the Arctic. Furthermore, this study highlights the need to assess heterogeneous reactions for a broad range of semivolatile persistent organic pollutants (POPs) and priority chemicals so that their fate and transport can be assessed and ultimately modeled more accurately.

■ ASSOCIATED CONTENT

Supporting Information

Experimental details, the details of the photochemical reactor reaction system, reactor, structures of OPEs, NIST mass spectra of OPEs studied in this work, stability of the aerosol source, and reactivity of TPhP for oxalic acid coated TPhP−AS. This material is available free of charge via the Internet at http://pubs.acs.org.

■ AUTHOR INFORMATION

Corresponding Author

*Phone: 1-416-739-4840; fax: 1-416-739-4281; e-mail: John.Liggio@ec.gc.ca.

Notes

The authors declare no competing financial interest.

■ ACKNOWLEDGMENTS

This research was financially supported by the Chemicals Management Plan (CMP) and the Clean Air Regulatory Agenda (CARA). The authors would like to thank Dr. Li Huang for fluid mechanics simulation during the design of the reactor.

■ REFERENCES

(1) Regnery, J.; Püttmann, W. Organophosphorus flame retardants and plasticizers in rain and snow from middle Germany. *Clean−Soil, Air, Water* **2009**, *37*, 334−342.

(2) The European Flame Retardants Association. Frequently asked questions on flame retardants. 2007, *16*, http://www.flameretardants-online.com/images/userdata/pdf/168_DE.pdf.
(3) Reemtsma, T.; García-López, M.; Rodríguez, I.; Quintana, J. B.; Rodil, R. Organophosphorus flame retardants and plasticizers in water and air I. Occurrence and fate. *Trends. Analyt. Chem.* **2008**, *27*, 727−737.
(4) Dodson, R. E.; Perovich, L. J.; Covaci, N. V.; den Eede, N. V.; Ionas, A. C.; Dirtu, A. C.; Brody, J. G.; Rudel, R. A. After the PBDE phase-out: A broad suite of flame retardants in repeat house dust samples from California. *Environ. Sci. Technol.* **2012**, *46*, 13056−13066.
(5) Regnery, J.; Püttmann, W. Seasonal fluctuations of organophosphate concentrations in precipitation and storm water runoff. *Chemosphere* **2010**, *78*, 958−964.
(6) Rodil, R.; Quintana, J. B.; Concha-Graña, E.; López-Mahía, P.; Muniatequi-Lorenzo, S.; Prada-Rodríguez, D. Emerging pollutants in sewage, surface and drinking water in Galicia (NW Spain). *Chemosphere* **2012**, *86*, 1040−1049.
(7) Martínez-Carballo, E.; González-Barreiro, C.; Sitka, A.; Scharf, S.; Gans, O. Determination of selected organophosphate esters in the aquatic environment of Austria. *Sci. Total Environ.* **2007**, *388*, 290−299.
(8) Mihajlović, I.; Miloradov, M. V.; Fries, E. Application of twisselmann extraction, SPME, and GC-MS to assess input sources for organophosphate esters into soil. *Environ. Sci. Technol.* **2011**, *45*, 2264−2269.
(9) Möller, A.; Sturm, R.; Xie, Z. Y.; Cai, M. H.; He, J. F.; Ebinghaus, R. Organophosphorus flame retardants and plasticizers in airborne particles over the Northern Pacific and Indian Ocean toward the polar regions: Evidence for global occurrence. *Environ. Sci. Technol.* **2012**, *46*, 3127−3134.
(10) Andresen, J. A.; Grundmann, A.; Bester, K. Organophosphorus flame retardants and plasticisers in surface waters. *Sci. Total Environ.* **2004**, *332*, 155−166.
(11) Regnery, J.; Püttmann, W. Occurrence and fate of organophosphorus flame retardants and plasticizers in urban and remote surface waters in Germany. *Water Res.* **2010**, *44*, 4097−4104.
(12) Matamoros, V.; Arias, C. A.; Nguyen, L. X.; Salvadó, V.; Brix, H. Occurrence and behavior of emerging contaminants in surface water and a restored wetland. *Chemosphere* **2012**, *88*, 1083−1089.
(13) Ali, N.; Dirtu, A. C.; den Eede, N. V.; Goosey, E.; Harrad, S.; Neels, H.; Mannetje, A.; Coakley, J.; Douwes, J.; Covaci, A. Occurrence of alternative flame retardants in indoor dust from New Zealand: Indoor sources and human exposure assessment. *Chemosphere* **2012**, *88*, 1276−1282.
(14) Möller, A.; Xie, Z.; Caba, A.; Sturm, R.; Ebinghaus, R. Organophosphorus flame retardants and plasticizers in the atmosphere of the North Sea. *Environ. Pollut.* **2011**, *159*, 3660−3665.
(15) Salamova, A.; Ma, Y.; Venier, M.; Hites, R. A. High levels of organophosphate flame retardants in the Great Lakes atmosphere. *Environ. Sci. Technol. Lett.* **2013**, DOI: dx.doi.org/10.1021/ez400034n.
(16) Verbruggen, E. M. J.; Rila, J. P.; Traas, T. P.; Posthuma-Doodeman, C. J. A. M.; Posthumus, R. *Environmental Risk Limits for Several Phosphate Esters, With Possible Application As Flame Retardant*; RIVM report 601501024, 2005.
(17) Aschmann, S. M.; Long, W. D.; Atkinson, R. Temperature-dependent rate constants for the gas-phase reactions of OH radicals with 1,3,5-trimethylbenzene, triethyl phosphate, and a series of alkylphosphonates. *J. Phys. Chem. A* **2006**, *110*, 7393−7400.
(18) Atmospheric Oxidation Program for Microsoft Windows (AOPWIN). U.S. Environmental Protection Agency, 2000.
(19) GDCh-Advisory Committee on Existing Chemicals of Envrionmental Relvance (BUA). *Di(2-ethylhexyl)phosphate, Tri(2-ethylhexyl)phosphate BUA Report 172.*, 1995.
(20) Atkinson, R.; Arey, J. Atmospheric degradation of volatile organic compounds. *Chem. Rev.* **2003**, *103*, 4605−4638.
(21) George, I. J.; Vlasenko, A.; Slowik, J. G.; Broekhuizen, K.; Abbatt, J. P. D. Heterogeneous oxidation of saturated organic aerosols by hydroxyl radicals: Uptake kinetics, condensed-phase products, and particle size change. *Atmos. Chem. Phys.* **2007**, *7*, 4187−4201.
(22) Veen, I. v. d.; Boer, J. d. Phosphorus flame retardants: Properties, production, environmental occurrence, toxicity and analysis. *Chemosphere* **2012**, *88*, 1119−1153.
(23) Saleh, R.; Donahue, N. M.; Robinson, A. L. Time scales for gas-particle partitioning equilibration of secondary organic aerosol formed from alpha-pinene ozonolysis. *Environ. Sci. Technol.* **2013**, *47*, 5588−5594.
(24) Meng, Z.; Seinfeld, J. H. Time scales to achieve atmospheric gas-aerosol equilibrium for volatile species. *Atmos. Environ.* **1996**, *30*, 2889−2900.
(25) Fuchs, N. A.; Sutugin, A. G. *Highly Dispersed Aerosols*; Butterworth-Heinemann: Newton, MA, 1970.
(26) Worsnop, D. R.; Morris, J. W.; Shi, Q.; Davidovits, P.; Kolb, C. E. A chemical kinetic model for reactive transformations of aerosol particles. *Geophys. Res. Lett.* **2002**, *29*, 1996, doi:10.1029/2002gl015542.
(27) Tuazon, E. C.; Atkinson, R.; Aschmann, S. M.; Arey, J.; Winer, A. M.; Pitts, J. N. Atmospheric loss processes of 1,2-dibromo-3-chloropropane and trimethyl phosphate. *Environ. Sci. Technol.* **1986**, *20*, 1043−1046.
(28) Aschmann, S. M.; Long, W. D.; Atkinson, R. Rate constants for the gas-phase reactions of OH radicals with dimethyl phosphonate over the temperature range of 278−351 K and for a series of other organophosphorus compounds at ∼280 K. *J. Phys. Chem. A* **2008**, *112*, 4793−4799.
(29) Burns, D. S.; Cory, M. G.; Taylor, D. E; Bunte, S. W.; Runge, K.; Vasey, J. L. A comparison of primary and secondary hydrogen abstraction from organophosphates by hydroxyl radical. *Int. J. Chem. Kinet.* **2013**, *45*, 187−201, doi:10.1002/kin.20755.
(30) Kawagoshi, Y.; Nakamura, S.; Fukunaga, I. Degradation of organophosphoric esters in leachate from a sea-based solid waste disposal site. *Chemosphere* **2002**, *48*, 219−225.
(31) Watts, M. J.; Linden, K. G. Photooxidation and subsequent biodegradability of recalcitrant tri-alkyl phosphates TCEP and TBP in water. *Water Res.* **2008**, *42*, 4949−4954.
(32) Watts, M. J.; Linden, K. G. Advanced oxidation kinetics of aqueous trialkyl phosphate flame retardants and plasticizers. *Environ. Sci. Technol.* **2009**, *43*, 2937−2942.
(33) Atkinson, R. Kinetics and Mechanisms of the gas-phase reactions of the hydroxyl radical with organic compounds under atmospheric conditions. *Chem. Rev.* **1986**, *85*, 69−201.
(34) Kessler, S. H.; Smith, J. D.; Che, D. L.; Worsnop, D. R.; Wilson, K. R.; Kroll, J. H.. Chemical sinks of organic aerosol: Kinetics and products of the heterogeneous oxidation of erythritol and levoglucosan. *Environ. Sci. Technol.* **2010**, *44*, 7005−7010.
(35) Kessler, S. H.; Nah, T.; Daumit, K. E.; Smith, J. D.; Leone, S. R.; Kolb, C. E.; Worsnop, D. R.; Wilson, K. R.; Kroll, J. H. OH-initiated heterogeneous aging of highly oxidized organic aerosol. *J. Phys. Chem. A* **2012**, *116*, 6358−6365.
(36) Liu, C.; Zhang, P.; Wang, Y.; Yang, B.; Shu, J. Heterogeneous reactions of particulate methoxyphenols with NO_3 radicals: Kinetics, products, and mechanisms. *Environ. Sci. Technol.* **2012**, *46*, 13262−13269.
(37) Hearn, J. D.; Smith, G. D. A mixed-phase relative rates technique for measuring aerosol reaction kinetics. *Geophys. Res. Lett.* **2006**, *33*, L17805, doi:10.1029/2006gl026963.
(38) Lambe, A. T.; Zhang, J. Y.; Sage, A. M.; Donahue, N. M. Controlled OH radical production via ozone-alkene reactions for use in aerosol aging studies. *Environ. Sci. Technol.* **2007**, *41*, 2357−2363.
(39) Smith, J. D.; Kroll, J. H.; Cappa, C. D.; Che, D. L.; Liu, C. L.; Ahmed, M.; Leone, S. R.; Worsnop, D. R.; Wilson, K. R. The heterogeneous reaction of hydroxyl radicals with sub-micron squalane particles: A model system for understanding the oxidative aging of ambient aerosols. *Atmos. Chem. Phys.* **2009**, *9*, 3209−3222.
(40) Rudich, Y.; Donahue, N. M.; Mentel, T. F. Aging of organic aerosol: Bridging the gap between laboratory and field studies. *Annu. Rev. Phys. Chem.* **2007**, *58*, 321−352.

(41) Kuwata, M.; Martin, S. T. Phase of atmospheric secondary organic material affects its reactivity. *Proc. Natl. Acad. Sci. U.S.A.* **2012**, *109*, 17354−17359.
(42) Shiraiwa, M.; Ammann, M.; Koop, T.; Pöschl, U. Gas uptake and chemical aging of semisolid organic aerosol particles. *Proc. Natl. Acad. Sci. U.S.A.* **2011**, *108*, 11003−11008.
(43) Katrib, Y.; Biskos, G.; Buseck, P. R.; Davidovits, P.; Jayne, J. T. Ozonolysis of mixed oleic-acid/stearic-acid particles: Reaction kinetics and chemical morphology. *J. Phys. Chem. A* **2005**, *109*, 10910−10919.
(44) Kawamura, K.; Semere, R.; Imai, Y.; Fujii, Y.; Hayashi, M. Water soluble dicarboxylic acids and related compounds in Antarctic aerosols. *J. Geophys. Res.-Atmos.* **1996**, *101*, 18721−18728.
(45) Falkovich, A. H.; Graber, E. R.; Schkolnik, G.; Rudich, Y.; Maenhaut, W.; Artaxo, P. Low molecular weight organic acids in aerosol particles from Rondônia, Brazil, during the biomass-burning, transition and wet periods. *Atmos. Chem. Phys.* **2005**, *5*, 781−797.
(46) Stone, E. A.; Hedman, C. J.; Zhou, J.; Mieritz, M.; Schauer, J. J. Insights into the nature of secondary organic aerosol in Mexico City during the MILAGRO experiment 2006. *Atmos. Environ.* **2010**, *44*, 312−319.
(47) Zhou, S.; Lee, A. K. Y.; McWhinney, R. D.; Abbatt, J. P. D. Burial effects of organic coatings on the heterogeneous reactivity of particle-borne benzo[a]pyrene (BaP) toward ozone. *J. Phys. Chem. A* **2012**, *116*, 7050−7056.
(48) Prinn, R. G.; Huang, J.; Weiss, R. F.; Cunnold, D. M.; Fraser, P. J.; Simmonds, P. G.; McCulloch, A.; Harth, C.; Salameh, P.; O'Doherty, S.; Wang, R. H. J.; Porter, L.; Miller, B. R. Evidence for substantial variations of atmospheric hydroxyl radicals in the past two decades. *Science* **2001**, *292*, 1882−1888.
(49) Abramson, E.; Imre, D.; Beránek, J.; Wilson, J.; Zelenyuk, A. Experimental determination of chemical diffusion within secondary organic aerosol particles. *Phys. Chem. Chem. Phys.* **2013**, *15*, 2983−2991.
(50) Fenimore, C. P.; Jones, G. W. Oxidation of soot by hydroxyl radicals. *J. Phys. Chem.* **1967**, *71*, 593−597.